

Iron oxide impregnated sugarcane bagasse waste material as sorbent for As(III) removal from water: kinetic, equilibrium and thermodynamic studies

Ashish Nashine and Ajay Tembhurkar

ABSTRACT

Adsorption of arsenite (As(III)) from aqueous solutions onto iron oxide impregnated sugarcane bagasse was investigated in this study. The linear regression analysis showed that Langmuir adsorption isotherm fitted well to the experimental data. Langmuir constants 'a' related to the adsorption capacity and 'b' related to the binding energy of sorption system were found to be 1.55 mg/g and 46.44 L/mg, respectively. A kinetic study revealed that uptake of As(III) was rapid in the first 30 min after which it slowed down and became almost constant after 90 min, indicating that the equilibrium had been reached. Kinetic data correlated well with the pseudo-second order kinetic model, suggesting that the adsorption process might be chemisorption. Estimated pseudo-second order kinetic rate constant was 2.113 g/mg min. Evaluation of thermodynamic parameters (ΔG , ΔH , ΔS) indicated that the adsorption process was feasible and endothermic in nature.

Key words | adsorbent, adsorption, arsenic, isotherm, kinetic

Ashish Nashine (corresponding author)
Ajay Tembhurkar
Department of Civil Engineering,
Visvesvaraya National Institute of Technology,
Nagpur 440011,
India
E-mail: alnashine@gmail.com

INTRODUCTION

Arsenic in ground water has become a global matter of concern. In recent years, the problem has increased worldwide, including several regions of southeast Asia such as Bangladesh, several states of India, Nepal, Myanmar, Pakistan, Vietnam, Lao People's Democratic Republic, Cambodia, China (Mukherjee *et al.* 2006), Chile, Ghana, Hungary, Mongolia, Mexico, New Zealand, Philippines, Taiwan and in the lowlands of Sumatra in Indonesia (Winkel *et al.* 2008). Arsenic is toxic and has a carcinogenic element and ingestion causes various diseases such as dermatitis, hypertension, respiratory, neurologic and liver disorders (IARC 2004). To reduce arsenic related illness the United State Environmental Protection Agency and many countries have lowered the public drinking-water standard from 50 to 10 $\mu\text{g/L}$.

Conventionally, coagulation and flocculation, membrane filtration, ion exchange and adsorption processes are used for arsenic removal. Coagulation and flocculation, membrane filtration and ion exchange techniques require relatively high capital and operating costs. Alzheimer's disease and

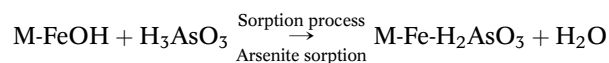
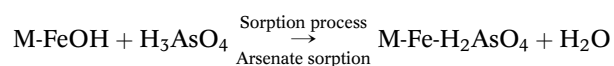
carcinogenic effects of coagulants alum lime, aluminum sulphate, polyaluminum chloride, polyaluminum silico sulphate, soda ash and synthetic polymers resulting from such treatments are other serious drawbacks of the coagulation and flocculation process (Pushpa *et al.* 2006). Membranes can be fouled by colloidal matter in the raw water, particularly organic matter. Iron and manganese can also lead to scaling and membrane fouling. It is widely recognized that adsorption is an ideal and appropriate technique compared to other techniques. Adsorption is a cheaper technique, simple in operation and maintenance is usually low. Many adsorbents such as activated carbon (Lorenzen *et al.* 1995; Wu *et al.* 2009), activated alumina (Singh & Pant 2004) have been used for arsenic removal, however dissolving of the aluminum is regarded as a human nerve toxin (Zhao *et al.* 2009). Commercial adsorbents are not suitable for developing countries because they are expensive.

Nowadays, research is devoted towards the study of natural or non-conventional adsorbents as they are cheap,

locally available and environmentally favorable. Regeneration may not be required and they can be disposed of safely. Very little study has been conducted for arsenic removal on adsorbents developed from natural materials. Cupressus female cone (Murugan & Subramanian 2004), shelled Moringa Oleifera Lamarck seed powder (Pushpa *et al.* 2006), laterite (Maiti *et al.* 2007), red soil (Nemade *et al.* 2009) and maize leaves (Kamsonlian *et al.* 2011) have been studied for arsenic removal from water. Also, various iron(III) oxides such as amorphous hydrous ferric oxide, poorly crystalline hydrous ferric oxide (Wilkie & Hering 1996) and goethite (Gimenez *et al.* 2007) were found to be effective adsorbent materials for the removal of arsenic from aqueous solutions. Iron oxides have a strong affinity for arsenic in water. However, they are available only as fine powders or are generated *in situ* as gels, which are difficult to separate from water after adsorption is completed (Guo *et al.* 2007; Habuda-Stanic *et al.* 2007). Hence, in the present study natural waste material sugarcane bagasse was identified as the adsorbent material and impregnated with iron oxide for enhanced removal of As(III), which was considered difficult to remove from water. The present study also deals with isotherm, kinetic and thermodynamic analysis for As(III) removal from the water on iron oxide impregnated sugarcane bagasse (IOISB) adsorbent.

MECHANISM OF ADSORPTION

The mechanism of arsenic adsorption on ferric oxide is associated with the formation of surface complexes between soluble arsenic species and the solid hydroxide surface sites. Ferric arsenate or ferric arsenite is produced due to arsenic contact with the deposited ferric oxides as presented in the following reactions (Solozhenkin *et al.* 2007):



These equations describe sorption of arsenic on ferric oxides on supports (M).

MATERIALS AND METHODS

Reagents and apparatus

All the chemicals used in the current study were of analytical grade. Stock solutions containing 1,000 mg/L of As(III) was prepared by dissolving As_2O_3 (SD Fine Chem., India) in distilled water. Working solutions as per the experimental requirements were freshly prepared from the stock solution. $\text{Fe}(\text{NO}_3)_3 \cdot 9\text{H}_2\text{O}$ (Merck) was used for the coating process. Quantitative determination of arsenic was carried out by the silver diethyl dithiocarbamate method using a UV-VIS spectrophotometer (Elico, India, Model no. SL 210) at a wavelength of 535 nm.

Preparation and characterization of adsorbent

Sugarcane bagasse was used for preparing adsorbent. Sugarcane bagasse was air-dried and crushed by a grinder. The biomass was sieved through a 2 mm copper sieve and 40 g of the crushed material was placed in a beaker and mixed with 400 mL of 1 N nitric acid. The mixer was heated on a hot plate maintaining a temperature of 70–80 °C for 20 min, cooled and washed with distilled water until the dirty color was removed. The washed biomass was then mixed with 400 mL of 1 N NaOH, heated again at 70–80 °C for 20 min and washed thoroughly. This material was air-dried for 3–4 days, grinded and sieved through a 600 micron sieve then the adsorbent was impregnated with iron oxide. A solution was prepared using ferric nitrate ($\text{Fe}(\text{NO}_3)_3 \cdot 9\text{H}_2\text{O}$) and sodium hydroxide. One mL of 10 M sodium hydroxide was mixed with 80 mL 2 M ferric nitrate, then 20 g of adsorbent was placed in a pot and the solution was poured slowly and homogenized by mixing thoroughly. The mixture was kept in an oven at 80 °C for 3 h. After 3 h the oven temperature was raised to 110 °C for another 24 h. The material was washed with distilled water, dried again in an oven at 80 °C for 24 h, sieved through a 600 micron sieve and stored in a capped bottle. The surface area of the adsorbent was measured using a Horiba SA series (Japan) BET (Brunauer–Emmett–Teller) surface area analyzer by nitrogen gas adsorption. The surface morphology of IOISB adsorbent was compared before and after adsorption by scanning electron microscopy (SEM).

Adsorption experiments

Batch adsorption experiments were conducted to obtain the data for the kinetic, equilibrium, and thermodynamic study for As(III) adsorption on IOISB adsorbent at room temperature. The experiment was conducted in glass beakers, containing As(III) solution having 0.380 mg/L initial concentration by varying adsorbent dose (0.5–10 g/L) to study the effect of IOISB adsorbent on As(III) removal. The suspensions were stirred for 60 min. For isotherm study, 10 g/L of the adsorbent was stirred with 250 mL of As(III) solutions having concentrations of 0.2, 0.5, 1.0, 1.5 and 2.0 mg/L. The suspensions were stirred for 90 min, which was the optimum contact time determined earlier, at 30 rpm. The kinetic study was conducted by varying contact time from 5 to 120 min. An adsorbent dose of 10 g/L was stirred with 250 mL of As(III) solutions in a series of beakers having a concentration of 0.395 mg/L at 30 rpm and room temperature. Similar experiments were carried out by varying temperature (283–313 K) at an adsorbent dose of 10 g/L, contact time of 90 min, pH 6, mixing speed of 50 rpm, keeping 0.5 mg/l initial As(III) concentration, which were the optimum values determined earlier. After stirring, suspensions were allowed to settle for 30 min and filtered. The filtrates were analyzed to estimate residual arsenic concentration after adsorption.

RESULTS AND DISCUSSION

Characterization of adsorbent

The BET surface area of the adsorbent was found to be 192.86 m²/g. Figure 1(a) and 1(b) shows the SEM image of

IOISB adsorbent before and after adsorption of As(III) ions. From Figure 1(a), it is observed that the adsorbent surface has a highly porous structure. This porous layer contributes to the significantly larger surface area. The adsorbent particles existed in clustered shapes and their actual size could not be determined. After adsorption of As(III), as seen in Figure 1(b), a reduction in the pore area of adsorbent is observed.

Effect of adsorbent dose

The effect of adsorbent dose on As(III) removal at an initial concentration of 0.380 mg/L is shown in Figure 2. The amount of As(III) adsorbed per unit weight of adsorbent 'q' (mg/g) decreased with an increase in adsorbent dose, while the percentage As(III) removal increased with an increase in adsorbent dose. There was no appreciable increase in percentage As(III) removal if the adsorbent dose was increased further. This might be due to the availability of more active sites with an increase in the adsorbent dose (Tembhurkar & Dongre 2006). A further increase of adsorbent does not have much affect due to the non-availability of adsorbate around the adsorbent. As(III) removal was 98.90% at 10 g/L adsorbent dose. The As(III) concentration after adsorption at an adsorbent dose of 10 g/L was 0.004 mg/L, which is below the WHO standards of 0.01 mg/L.

Adsorption isotherm

The adsorption isotherms were obtained to determine the capacity of the adsorbent for As(III) removal at room temperature. The adsorbate concentrations were varied from 0.2 to

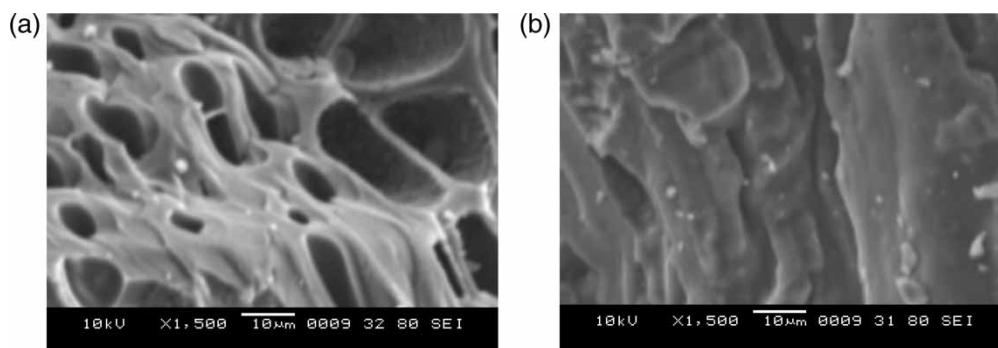


Figure 1 | Scanning electron micrographs of IOISB adsorbent before and after As(III) adsorption.

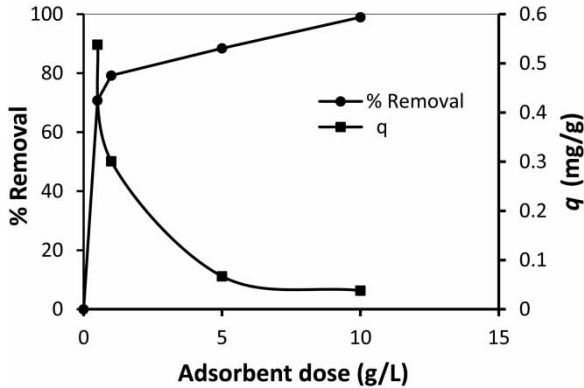


Figure 2 | Effect of adsorbent dose on As(III) adsorption (initial concentration of solution 0.380 mg/L, contact time 60 min, mixing speed 30 rpm).

2.0 mg/L keeping the adsorbent dose at 10 g/L, mixing time 90 min and speed 30 rpm. The pH of the adsorbate was 7.1. The amount of As(III) adsorbed increased linearly from 0.049 to 0.184 mg/g, when the initial concentration increased from 0.5 to 2.0 mg/L, as shown in Figure 3. This was because at a higher solute concentration the adsorption was greater due to increased concentration gradient (Maiti *et al.* 2007).

The experimental data obtained are applied to the Langmuir and the Freundlich models.

The Freundlich isotherm is expressed as:

$$q_e = k C_e^{1/n} \quad (1)$$

$$\log q_e = \log k + \frac{1}{n} \log C_e \quad (2)$$

and the Langmuir isotherm as:

$$\frac{1}{q_e} = \frac{1}{abC_e} + \frac{1}{a} \quad (3)$$

where C_e is the equilibrium solute concentration (mg/L), q_e is the amount of As(III) adsorbed at equilibrium (mg/g), k and n are the Freundlich constants representing the adsorption capacity (mg/g) and the adsorption intensity. Larger values of k mean larger capacity of adsorption. Larger values of $1/n$ mean that the adsorption bond is weak because the value of q_e experiences large changes for small changes in C_e . The values of the constants ' n ' and ' k ' can be determined from the slope and intercept of the plot between $\log q_e$ and $\log C_e$. a and b are Langmuir constants related to adsorption

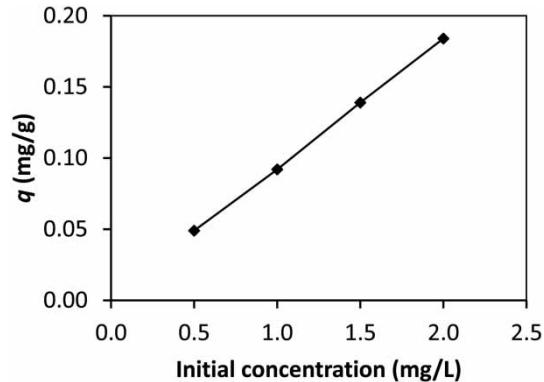


Figure 3 | Effect of initial adsorbate conc. on As(III) adsorption (adsorbent dose 10 g/L, contact time 90 min, mixing speed 30 rpm).

capacity and binding energy of the sorption system (L/mg). The constants ' b ' and ' a ' are calculated from the slope and intercept of the plot between $1/q_e$ and $1/C_e$.

The experimental data plotted for the Freundlich isotherm and the Langmuir isotherm are shown in Figures 4 and 5. The constants for both models along with regression coefficients (R^2) are summarized in Table 1. The values of correlation coefficient (R^2) suggest that both Langmuir and Freundlich isotherms fit the adsorption data adequately. The results suggest that adsorption of As(III) removal on IOISB is a complex mechanism where the controlling step of arsenic adsorption is by both the surface adsorption and intra-particle pore diffusion. Singh & Pant (2004) and Maiti *et al.* (2007) have also reported that adsorption of As(III) on activated alumina and natural laterite follows both the isotherm models.

The dimensionless equilibrium parameter RL is estimated by the following equation to determine if the As(III)

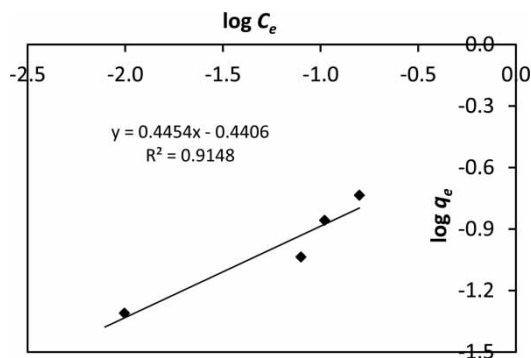


Figure 4 | Freundlich isotherm plot for adsorption of As(III) (adsorbent dose 10 mg/L, contact time 90 min, mixing speed 30 rpm).

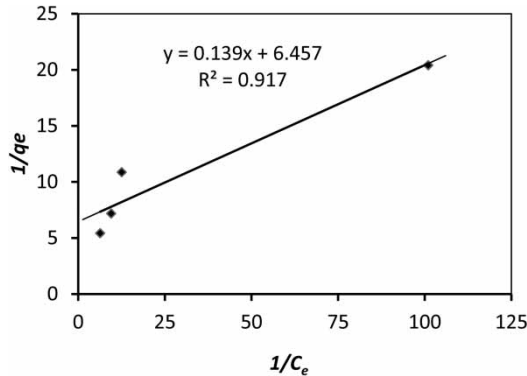


Figure 5 | Langmuir isotherm plot for adsorption of As(III) (adsorbent dose 10 mg/L, contact time 90 min, mixing speed 30 rpm).

Table 1 | Adsorption isotherm parameters for As(III) adsorption on IOISB adsorbent

	k (mg/g)	N	a (mg/g)	b (L/mg)	R^2
Freundlich isotherm	0.363	2.247	–	–	0.914
Langmuir isotherm	–	–	0.155	46.44	0.917

adsorption process by IOISB is favorable or unfavorable for the Langmuir type adsorption process:

$$R_L = \frac{1}{1 + bC_o} \quad (4)$$

where C_o is the initial As(III) concentration and b is the Langmuir isotherm constant. The value of $R_L < 1$ represents the favorable adsorption and $R_L > 1$ describes unfavorable adsorption (Singh & Pant 2004).

Values of R_L at different concentrations as shown in Figure 6 are less than 1 representing the favorable

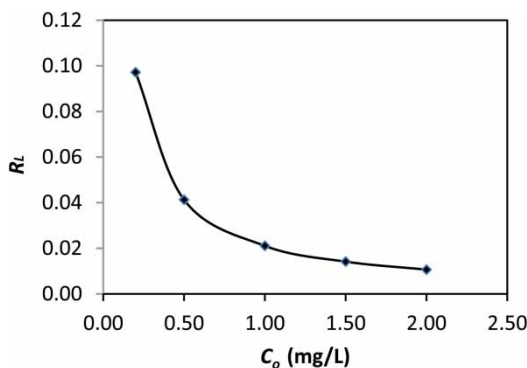


Figure 6 | Factor R_L for As(III) adsorption onto IOISB (adsorbent dose 10 mg/L, contact time 90 min, mixing speed 30 rpm).

adsorption of As(III) on IOISB adsorbent. Figure 6 also reveals that lower R_L values are obtained at higher As(III) concentrations, indicating a higher removal efficiency of IOISB adsorbent at higher As(III) concentrations.

Kinetic study

The kinetic study for As(III) adsorption on IOISB adsorbent was conducted by varying contact time from 5 to 120 min. at 10 g/L adsorbent dose, 0.395 mg/L initial concentration and room temperature (31 °C). It was found that As(III) uptake increased with an increase in contact time. The adsorption of As(III) was rapid in the first 30 min, after which it slowed down and became almost constant after 90 min, indicating that the equilibrium had been reached. Initially the sorbent sites were vacant, hence uptake was increasing with the lapse of time. Later, the number of sites decreased and ultimately the saturation of adsorbent sites occurred after a longer period of operation (Tembhurkar & Dongre 2006). About 99.24% removal of As(III) was achieved at 90 min contact time. Reported equilibrium time for As(III) adsorption are 2 h on iron oxide coated cement (Kundu & Gupta 2006), 2.5 h on natural laterite (Maiti *et al.* 2007), 20 h on polymeric Al/Fe modified montmorillonite (Ramesh *et al.* 2007) and 22 h on iron impregnated potato peels (Godbole & Dhoble 2011) adsorbents.

To estimate the uptake rate two kinetic models were analyzed from the data obtained. The pseudo-first order rate model is given by the following expression:

$$\log(q_e - q_t) = \log q_e - \left(\frac{k_1}{2.303}\right)t \quad (5)$$

where q_e and q_t (mg/g) are the amounts of arsenic adsorbed at equilibrium and time t (min), k_1 is the rate constant of the equation (min^{-1}). The value of k_1 is calculated from the slope of the linear plot of $\log(q_e - q_t)$ versus t , which is shown in Figure 7.

The pseudo-second order rate model is expressed as:

$$\frac{t}{q_t} = \frac{1}{h} + \left(\frac{1}{q_e}\right).t \quad (6)$$

where $h = k_2 q_e^2$ which denotes the initial sorption rate (mg/g min) and k_2 (g/mg min) is the rate constant of the pseudo-second order equation. The second order rate constant k_2 and q_e are calculated from the intercept and slope of the plot of t/q_t versus t . The experimental data plotted is shown in Figure 8. The calculated values of q_e , k_1 , k_2 and R^2 are presented in Table 2. The experimental q_e value is in agreement with the calculated q_e value and the plots show good linearity with an R^2 value of 0.983. This indicates that the pseudo-second order kinetic model

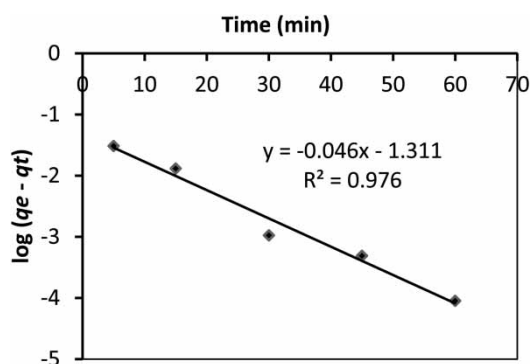


Figure 7 | First order kinetic model (adsorbent dose 10 g/L, initial concentration 0.395 mg/L, mixing speed 30 rpm).

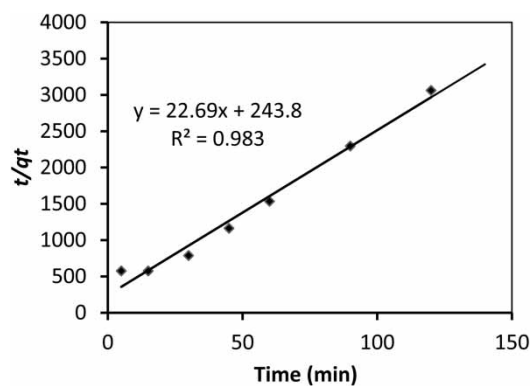


Figure 8 | Second order kinetic model (initial concentration 0.395 mg/L, adsorbent dose 10 g/L, mixing speed 30 rpm).

Table 2 | Kinetic parameters for As(III) adsorption on IOISB adsorbent

Temp (K)	Pseudo-first order parameters		Pseudo-second order parameters				
	k_1 (min ⁻¹)	R^2	h (mg/g min)	k_2 (g/mg min)	Experimental q_e (mg/g)	Calculated q_e (mg/g)	R^2
304	0.1059	0.976	0.0041	2.113	0.0392	0.0441	0.983

better represents the adsorption kinetics, suggesting that the adsorption process might be chemisorption. Some of the previous researchers also reported that pseudo-second order model correlates well to the experimental data obtained for the adsorption of As(III) on polymeric Al/Fe modified montmorillonite (Ramesh *et al.* 2007), fly ash agglomerates (Polowczyk *et al.* 2010) and maize leaves (Kamsonlian *et al.* 2011).

Thermodynamic study

The thermodynamic study for the adsorption of As(III) onto IOISB adsorbent was conducted in the temperature range of 10–40 °C at an initial adsorbate concentration of 0.5 mg/L and adsorbent dose of 10 g/L. It was found that the adsorption capacity increased with increasing temperature. The increase in adsorption capacity at higher temperatures may be due to the enlargement of pore size, i.e. a change in the surface properties of the adsorbent and/or activation of the adsorbent surface (Zeng 2004; Ramesh *et al.* 2007; Kamsonlian *et al.* 2011). The increase in adsorption with temperature may also be attributed to the decrease in the thickness of the boundary layer surrounding it, so that the mass transfer resistance of adsorbate in the boundary layer decreases. The possibility of adsorbent diffusion of solute within the pores at higher temperatures may not be ruled out. Since diffusion is an endothermic process, greater adsorption is observed at higher temperature (Wu *et al.* 2009).

Table 3 | Estimated thermodynamic parameters (ΔH , ΔG and ΔS) for As(III) adsorption onto IOISB adsorbent at different temperatures

Temperature (K)	ΔG (kJ/mol)	ΔH (kJ/mol)	ΔS (J/mol K)	R^2
283	-763.305	8,030.49	30.71	0.963
293	-928.983			
303	-1,375.37			
313	-1,649.89			

Table 4 | Comparison of efficiency of various adsorbents

Sr. no.	Adsorbent	Operating conditions				Efficiency %	Authors
		Ads. dose (g/L)	Initial conc. (mg/L)	Time (h)			
1	IOISB	10	0.395	1.5	99.24	Current study	
2	Iron treated A.C.	2	0.05	24	60.00	Payne & Abdel-Fattah (2005)	
3	Iron treated Chabazite	2	0.05	24	30.00	Payne & Abdel-Fattah (2005)	
4	Iron oxide-coated sand	–	0.1	12	73.2	Ramakrishna <i>et al.</i> (2006)	
5	Natural laterite	40	1.0	2.5	98.00	Maiti <i>et al.</i> (2007)	
6	Industrial waste – iron chips	10	0.5	1.0	92.00	Zhang <i>et al.</i> (2008)	
7	Iron impregnated coconut shell A.C.	1	0.2	–	89.00	Khare & Kumar (2011)	
8	Iron impregnated potato peels	20	1.0	22	99.27	Godbole & Dhoble (2011)	
9	Iron-oxide-coated natural rock	13	0.6	6	98.50	Maji <i>et al.</i> (2012)	

The equilibrium partition coefficient (K_c) is calculated as:

$$K_c = \frac{C_s}{C_e} \quad (7)$$

The thermodynamic parameters such as change in free energy (ΔG), enthalpy (ΔH) and entropy (ΔS) are calculated from the following equations and are given in Table 4.

$$\Delta G = -RT \ln K_c \quad (8)$$

$$\ln K_c = \frac{\Delta S}{R} - \frac{\Delta H}{RT} \quad (9)$$

where R is the gas constant (8.314 J/mol K), C_s and C_e are the equilibrium concentrations of the arsenic in the adsorbent (mg/L) and solution (mg/L) respectively and T is the solution temperature (K). ΔH and ΔS are calculated from the slope and intercept of the plot of $\ln K_c$ versus $1/T$ as shown in Figure 9. The estimated values of thermodynamic parameters are shown in Table 3. The negative ΔG values confirm the feasibility of the adsorption process and the spontaneous nature of As(III) adsorption onto IOISB adsorbent. The more negative values of ΔG with the rise in temperature imply a greater driving force to the adsorption process and show an increase in feasibility of adsorption at higher temperatures (Ramesh *et al.* 2007). A positive value of ΔH indicates endothermic nature of As(III) adsorption on to the adsorbent, whereas the positive value of ΔS indicates that the randomness increased with temperature during the adsorption of arsenic onto IOISB adsorbent.

The efficiency of IOISB and other adsorbents reported in literature are shown in Table 4.

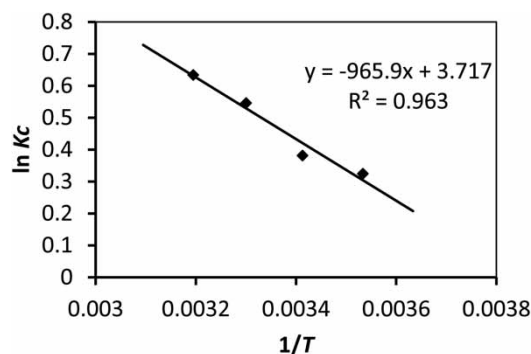


Figure 9 | Estimation of thermodynamic parameters (adsorbent dose 10 g/L, initial concentration 0.5 mg/L, contact time 90 min, mixing speed 50 rpm, pH 6).

CONCLUSIONS

IOISB was found to be a suitable adsorbent for As(III) removal from drinking water. It was found that the maximum adsorption of 98.90% occurs within 90 min of the operation, at an adsorbent dose of 10 g/L, contact time of 90 min, and mixing speed of 50 rpm, when initial adsorbate concentration, pH and room temperature were 0.5 mg/L, 6 and 30 °C, respectively. Linear regression analysis showed that both Freundlich and Langmuir isotherms fitted the adsorption data adequately. The adsorption process followed a pseudo-second order kinetic model. The result of the kinetic adsorption model reveals that the adsorption of As(III) onto IOISB adsorbent was because of chemisorptions. The negative ΔG values obtained from the experimental results confirm the feasibility and spontaneous nature of the adsorption. Positive values of both ΔH and ΔS indicate the endothermic nature of

the process with increased randomness at the liquid–solid interface during As(III) ion adsorption in batch studies.

REFERENCES

- Gimenez, J., Martinez, M., de Pablo, J., Rovira, M. & Duro, L. 2007 Arsenic sorption onto natural hematite, magnetite, and goethite. *J. Hazard. Mater.* **141**, 575–580.
- Godbole, B. J. & Dhoble, R. M. 2011 Removal of As(III) from groundwater by iron impregnated potato peels (IIPP): batch study. *Int. J. Adv. Eng. Sci. Technol.* **7** (1), 54–64.
- Guo, H., Stuben, D. & Berner, Z. 2007 Removal of arsenic from aqueous solution by natural siderite and hematite. *Appl. Geochem.* **22**, 1039–1051.
- Habuda-Stanic, M., Mirko, K., Brankica, K. & Zeljka, R. 2007 Arsenic and arsenate sorption by hydrous ferric oxide/polymeric material. *Desalination* **229**, 1–9.
- IARC (International Agency for Research on Cancer) 2004 *Some Drinking Water Disinfectants and Contaminants Including Arsenic*, monograph 84. IARC, Lyons, France.
- Kamsonlian, S., Balomajumder, C. & Chand, S. 2011 Removal of As(III) from aqueous solution by biosorption onto maize (*Zea mays*) leaves surface: parameters optimization, sorption isotherm, kinetic and thermodynamics studies. *Res. J. Chem. Sci.* **1** (5), 73–79.
- Khare, P. & Kumar, A. 2011 Arsenic removal from water using iron impregnated activated carbon. In *Proceedings of International Conference on Recent Advances in Chemical Engineering and Technology*, 10–12 March, Kochi, India.
- Kundu, S. & Gupta, A. K. 2006 Adsorptive removal of As(III) from aqueous solution using iron oxide coated cement (IOCC): evaluation of kinetic, equilibrium and thermodynamic models. *Separ. Purif. Technol.* **51**, 165–172.
- Lorenzen, L., Van Deventer, J. S. J. & Landi, W. M. 1995 Factors affecting the mechanism of the adsorption of arsenic species on activated carbon. *Miner. Eng.* **8** (4/5), 557–569.
- Maiti, A., Dasgupta, S., Basu, J. K. & De, S. 2007 Adsorption of arsenite using natural laterite as adsorbent. *Separ. Purif. Technol.* **55**, 350–359.
- Maji, S. K., Kao, Y.-H., Wang, C.-J., Lu, G.-S., Wu, J.-J. & Liu, C.-W. 2012 Arsenic removal from real arsenic-bearing groundwater by adsorption on iron-oxide-coated natural rock (IOCNR). *Chem. Eng. J.* **203**, 285–293.
- Mukherjee, A., Sengupta, M. K. & Hossain, M. A. 2006 Arsenic contamination in groundwater: a global perspective with emphasis on the Asian scenario. *J. Health Popul. Nutr.* **24**, 142–163.
- Murugan, M. & Subramanian, E. 2004 An efficient and reversible sorptive removal of arsenic (III) from aqueous solution by the biosorbent cupressus female cone. *Indian J. Chem. Technol.* **11**, 304–308.
- Nemade, P. D., Kadam, A. M. & Shankar, H. S. 2009 Adsorption of arsenic from aqueous solution on naturally available red soil. *J. Environ. Biol.* **30** (4), 499–504.
- Payne, K. B. & Abdel-Fattah, T. M. 2005 Adsorption of arsenate and arsenite by iron-treated activated carbon and zeolites: effects of pH, temperature, and ionic strength. *J. Environ. Sci. Health* **40**, 723–749.
- Polowczyk, I., Bastrzyk, A., Kozlecki, T., Sawinski, W., Rudnicki, P., Sokołowski, A. & Sadowski, Z. 2010 Use of Fly ash agglomerates for removal of arsenic. *Environ. Geochem. Health* **32**, 361–366.
- Pushpa, K., Parul, S., Shalini, S. & Shrivastava, M. M. 2006 Biosorption studies on shelled moringa oleifera lammark seed powder: removal and recovery of arsenic from aqueous system. *Int. J. Miner. Process.* **78**, 131–139.
- Ramakrishna, D. M., Viraraghavan, T. & Jin, Y.-C. 2006 Iron oxide coated sand for arsenic removal: investigation of coating parameters using factorial design approach. *Practice Periodical of Hazardous, Toxic, and Radioactive Waste Management*, ASCE, October, pp. 198–206.
- Ramesh, A., Hasegawa, H., Maki, T. & Ueda, K. 2007 Adsorption of inorganic and organic arsenic from aqueous solutions by polymeric Al/Fe modified montmorillonite. *Separ. Purif. Technol.* **56**, 90–100.
- Singh, T. S. & Pant, K. K. 2004 Equilibrium kinetics and thermodynamic studies for adsorption of As(III) on activated alumina. *Separ. Purif. Technol.* **36** (2), 139–147.
- Solozhenkin, P. M., Zouboulis, A. I. & Katsoyiannis, I. A. 2007 Removal of arsenic compounds by chemisorption filtration. *J. Mining Sci.* **43** (2), 212–220.
- Tembhurkar, A. R. & Dongre, S. 2006 Studies on fluoride removal using adsorption process. *J. Environ. Sci. Eng.* **48** (3), 151–156.
- Wilkie, J. A. & Hering, J. G. 1996 Adsorption of arsenic onto hydrous ferric oxide: effects of adsorbate/adsorbent ratios and co-occurring solutes. *Colloids Surf. Physicochem. Eng. Asp.* **107**, 97–110.
- Winkel, L., Berg, M. & Stengel, C. 2008 Hydrogeological survey assessing arsenic and other groundwater contaminants in the lowlands of Sumatra, Indonesia. *Appl. Geochem.* **23** (11), 3019–3028.
- Wu, Y. H., Li, B., Feng, S. X., Mi, X. M. & Jiang, J. L. 2009 Adsorption of Cr(VI) and As(III) on coaly activated carbon in single and binary systems. *Desalination* **249**, 1067–1073.
- Zeng, L. 2004 Arsenic adsorption from aqueous solutions on an Fe(III)-Si binary oxide adsorbent. *Water Qual. Res. J. Can.* **39** (3), 267–275.
- Zhang, R., Sun, H. & Yin, J. 2008 Arsenic and chromate removal from water by iron chips – effects of anions. *Front. Environ. Sci. Eng. China* **2** (2), 203–208.
- Zhao, Y., Huang, M., Wu, W. & Jin, W. 2009 Synthesis of the cotton cellulose based Fe(III)-loaded adsorbent for arsenic(V) removal from drinking water. *Desalination* **249**, 1006–1011.